EBioMedicine 67 (2021) 103370

Contents lists available at ScienceDirect

EBioMedicine

journal homepage: www.elsevier.com/locate/ebiom

Research paper

TNAP is a novel regulator of cardiac fibrosis after myocardial infarction by mediating TGF-β/Smads and ERK1/2 signaling pathways

Xiaocheng Cheng[a], Liyou Wang[a,b], Xuesong Wen[a], Lei Gao[a], Guoxing Li[a], Guanglei Chang[a], Shu Qin[a], Dongying Zhang[a,*]

[a] Department of Cardiology, the First Affiliated Hospital of Chongqing Medical University, Chongqing, 400016, China
[b] The Second Ward of Cardiovascular Medicine Department, Ankang City Central Hospital, Ankang, China

ARTICLE INFO

Article History:
Received 4 October 2020
Revised 4 April 2021
Accepted 15 April 2021
Available online xxx

Keywords:
TNAP
Myocardial infarction
Cardiac fibrosis
TGF-β1/Smads
ERK1/2

ABSTRACT

Background: Cardiac fibrosis is the most important pathogenesis leading to cardiac remodeling and heart failure after myocardial infarction (MI). Tissue nonspecific alkaline phosphatase (TNAP) has recently been recognized as a potential prognostic factor for MI. Nevertheless, the role of TNAP in cardiac fibrosis after MI has not been explicitly delineated.

Methods: A systematic review and meta-analysis was conducted to assess the effect of serum TNAP levels on mortality in patients with ischemic heart disease (IHD). A correlation analysis was performed to investigate the relationship between serum levels of TNAP and biomarkers of fibrosis. Heart biopsies from patients with MI and a mouse model of MI were used to detect the expression and distribution of TNAP. Furthermore, we established adenovirus-mediated knockdown and overexpression of TNAP, using a combination of in vivo and in vitro studies in mice, to determine the role and mechanism of TNAP in cardiac fibrosis after MI. In the in vitro studies, cardiac fibroblasts were cultured on soft plates.

Findings: After searching the main databases and performing a detailed assessment of the full-text articles, eight studies with 14,816 individuals were included in the quantitative analysis. We found that a high serum TNAP level was associated with an increased risk of mortality in patients with IHD and MI. The correlation analysis revealed a positive correlation between serum TNAP levels and the concentration of fibrosis biomarkers (PICP/PIIINP). The expression of TNAP was upregulated in the myocardium of patients with MI and in a mouse model of MI, accompanied by fibroblast activation and the deposition of collagen fibers. In the in vivo study, TNAP knockdown ameliorated cardiac fibrosis and improved cardiac function in mice. TNAP overexpression aggravated cardiac fibrosis and worsened cardiac function. In the in vitro study, TNAP promoted cardiac fibroblast differentiation, migration and proliferation. Mechanistically, the pro-fibrotic effect of TNAP on cardiac fibroblasts was at least partially achieved by activating the TGF-β1/Smads and ERK1/2 signaling pathways.

Interpretation: Based on these findings, TNAP plays an important pro-fibrotic role in cardiac fibrosis after MI by activating TGF-β/Smads and ERK1/2 signaling, indicating that it functions as a potential regulator of and therapeutic target in cardiac fibrosis.

Funding: This work was supported by the National Natural Science Foundation of China.

1. Introduction

Myocardial infarction (MI) persists as one of the leading causes of morbidity and mortality. Although advances in procedural and pharmaceutical strategies have improved the major adverse events after MI, the overall disease burden after MI remains unacceptably high [1]. The excessive deposition of extracellular matrix in the myocardial interstitium after MI induced by the loss of cardiomyocytes contributes to cardiac fibrosis [2]. The fibrotic reaction increases the stiffness of the myocardium, promotes the remodeling of the ventricular structure, and ultimately leads to systolic, diastolic dysfunction and heart failure [3].

Tissue nonspecific alkaline phosphatase (TNAP), a member of the phosphatase family, is usually expressed on the surface of mesenchymal stromal cells (MSCs) [4]. As a surface marker of MSCs, it is widely distributed in various human tissues. TNAP is a pivotal regulator molecule of bone and vascular calcification that promotes the

* Corresponding author at: Department of Cardiology, the First Affiliated Hospital of Chongqing Medical University, No.1 youyi street, Yuzhong district, Chongqing 400016, China.
E-mail address: zhangdongying@cqmu.edu.cn (D. Zhang).

https://doi.org/10.1016/j.ebiom.2021.103370

Research in context

Evidence before this study

Cardiac fibrosis is the most important pathogenesis leading to cardiac remodeling and heart failure after myocardial infarction (MI). Tissue nonspecific alkaline phosphatase (TNAP), a pivotal regulator molecule of bone and vascular calcification, is crucial in promoting the differentiation and metabolism of various cells. Recently, TNAP has recently been recognized as a potentially prognostic factor involved in patients with MI. Nevertheless, the role of TNAP in cardiac fibrosis after MI is still controversial.

Added value of this study

In this study, we found that a high serum TNAP level was associated with an increased risk of mortality in patients with ischemic heart diseases, and it was positive correlated with the concentration of PICP/PIIINP in patients with MI. The expression of TNAP was upregulated in the myocardium of patients with MI and in a mouse model of MI. Importantly, in the in vivo study, we found that TNAP knockdown ameliorated cardiac fibrosis and improved cardiac function in mice. In contrast, TNAP overexpression aggravated cardiac fibrosis and worsened cardiac function. In the in vitro study, TNAP promoted cardiac fibroblasts differentiation, migration and proliferation. TGF-β1/Smads and ERK1/2 signaling pathways partially mediate the role of TNAP in cardiac fibrosis after MI.

Implications of all the available evidence

TNAP plays an important pro-fibrotic role in cardiac fibrosis after MI, suggesting that TNAP may be a potential regulator and therapeutic target in cardiac fibrosis. Our data explored a new explanation for TNAP-related mortality after MI in addition to vascular calcification. These findings have potential clinical applications.

differentiation and metabolism of adipocytes, neurons and vascular smooth muscle cells [4–6]. Several studies have reported that the serum TNAP level may be associated with increased major adverse events in individuals with ischemic heart disease (IHD) [7,8].

The possible mechanism is that TNAP regulates the metabolism of calcium and phosphorus and may affect the prognosis of patients with MI by aggravating coronary artery calcification. However, this hypothesis is still controversial [9]. Tonelli et al. reported an association between a high serum TNAP level and an increased risk of heart failure in patients with MI [7]. Cardiac fibrosis after MI is one of the main causes of heart failure and death. Nevertheless, the role of TNAP in the progression of cardiac fibrosis after MI has not been explicitly elucidated [10,11]. Arnò et al. reported that TNAP limits the extent of cardiac fibrosis induced by Ang II by inactivating the TGF-/Smads signaling pathway [10]. However, Rodionov et al. found that TNAP overexpression in the endothelium resulted in significant cardiac systolic dysfunction and aggravated cardiac fibrosis in mice [11].

As shown in our recent study, TNAP inhibition by tetramisole attenuates cardiac fibrosis after MI in rats by deactivating TGF-β1/Smad2 signaling and activating P53 signaling pathways [12]. However, considering the multiple biological actions of tetramisole [13,14], the evidence that TNAP regulates cardiac fibrosis may not be sufficiently convincing. To further explore the role of TNAP in cardiac fibrosis, we first determined the relationship between the serum TNAP level and mortality in patients with IHD. In addition, we conducted a correlation analysis between the levels of serum TNAP and cardiac fibrosis biomarkers. Furthermore, we established adenovirus mediated-specific knockdown and overexpression of TNAP, using a combination of in vivo and in vitro studies in C57BL/6 J mice, to further determine the role and mechanism of TNAP in cardiac fibrosis after MI.

2. Materials and methods

2.1. Systematic review and meta-analysis

We conducted a comprehensive online search of published literature in the Medline, Cochrane and EMBASE databases (to December 31, 2020) to identify all publications and to assess the effect of serum TNAP levels on mortality in patients with IHD. The search strategy employed relevant keywords, including alkaline phosphatase, ischemic heart disease, myocardial infarction, and coronary artery disease. The search was limited to English language publications. Studies were included in this systematic review and meta-analysis if they met the following criteria: the exposures were alkaline phosphatase and the outcome was risks of cardiovascular mortality or all-cause mortality. Search results were reviewed by two investigators (C.X. and W.L.) who were required to be in agreement regarding study selection. Any discrepancies were resolved by discussion.

This systematic review and meta-analysis adhered to the Preferred Reporting Items for Systematic Reviews and Meta-Analyses (PRISMA) guidelines for pooled analyses of interventional studies [15]. Data were extracted by the two authors (C.X. and W.L), who independently used a predefined, standardized protocol and data collection instrument. Data on the study design, sample size, demographic characteristics, medical history of participants, follow-up time, serum TNAP level and outcomes were recorded. If multiple quantiles of serum TNAP levels were reported, quantitative analysis only included the highest and lowest quartiles of serum TNAP levels. The primary endpoints were all-cause mortality and cardiovascular mortality. The Newcastle–Ottawa Quality Assessment Scale (NOS) for observational trials was used to evaluate the quality of the study [16]. The NOS scale consists of eight questions with nine possible points. The quality of the included studies was independently assessed by the two review authors.

2.2. Correlation analysis

We performed a correlation analysis between serum TNAP levels and cardiac fibrosis biomarkers, including type I procollagen carboxy-terminal propeptide (PICP) and N-terminal propeptide of type III procollagen (PIIINP) [17]. Briefly, we recruited consecutive patients who underwent coronary angiography (March 1, 2019 to August 30, 2019). Thirty-one patients with acute MI (< 2 weeks) and 28 patients with negative findings were included. The detailed exclusion criteria are described in **Supplemental Table 1**. Fasting venous blood samples were drawn from the included individuals. The plasma tube containing EDTA was centrifuged immediately and the plasma aliquots were stored at −80 °C until final analysis without any freeze-thaw cycles. The serum TNAP concentration was analysed using a commercially available ELISA kit (A059–2, JianCheng Bioengineering Institute, Nanjing, China).

2.3. Human heart samples, mouse model of MI and animal studies

Five human heart specimens were obtained from donors who died from acute MI (< 2 weeks). Patients or patients' family members provided informed written consent prior to the inclusion of samples from these subjects. Specific pathogen free (SPF) male C57BL/6 J mice (6–8 weeks) were obtained from the experimental animal center of Chongqing Medical University, and raised in SPF animal experiment room (constant temperature of 20 ± 3 °C with 55% ± 10% humidity

and 12 h light/dark cycle). The model of MI was established as described below. Mice were anaesthetized with intraperitoneal injection of sodium pentobarbital (60 mg/kg), and additional doses were administered if necessary. Mice were intubated with a 25-gage endotracheal tube, and ventilation was performed at a rate of 180−220 breaths/min. The intercostal muscle was cut with an electrocautery pen, and the ribs were retracted to expose the heart. Then, the left anterior descending coronary artery (LAD) was permanently ligated with 8−0 nylon sutures at approximately 1.0−2.0 mm below the border between the left atrium and the left ventricle. The sham-operated mice underwent an identical operation as the MI group but without ligation of the LAD. Subsequently, mice were sacrificed at 3, 7, 14, 21 or 28 days after MI by isoflurane (5%) administration and cervical dislocation.

2.4. Knockdown and overexpression of TNAP in mice

Adenoviruses carrying a small hairpin RNA targeting TNAP (TNAP knockdown, adv-shTNAP) and the TNAP cDNA (TNAP overexpression, adv-TNAP-OE) were commercially constructed and synthesized using the BLOCK-iT Adenoviral RNAi Expression System (Hanbio Biotechnology Co., Ltd., China). The mouse adv-TNAP-shRNA targeting sequence was 5′- CACCTTGACTGTGGTTACTGCTGAT −3′. Mice were randomly assigned to control and experimental groups (n = 20 each group) according to a computer-generated sequence. When MI surgery was performed, adenoviruses were delivered into mice via in situ multipoint injection of the left ventricular anterior wall (50×10^{11} p.f.u. viruses per mouse). Control mice were injected with the negative adv-scramble or adv-GFP using the same protocol. Two weeks after MI was established, mice were sacrificed for subsequent experiments.

2.5. Echocardiographic assessment of cardiac function

Transthoracic echocardiography (IE33; Philips, Holland) was performed to assess cardiac function. Mice were anaesthetized by isoflurane inhalation (2−2.5%), and then isoflurane (1.5−2.0%) was administered throughout the procedure to maintain the heart rate between 450 and 550 beats/min. A two-dimensional parasternal short axis view was used to image the heart, and an M-mode echocardiogram was recorded at the papillary muscle level. Cardiac function parameters, such as the left ventricular ejection fraction (LVEF), fractional shortening (FS), left ventricular internal diameter at diastole (LVIDd) and left ventricular internal diameter at systole (LVIDs), were measured by the same investigator who was blinded to the groups.

2.6. Histological examination

The heart tissue was fixed with 4% paraformaldehyde, overnight at 4 °C and dehydrated by washes with ethanol. Subsequently, heart tissue was cut into 4 μm longitudinal sections and stained with Masson's trichrome or used for immunohistochemistry. Masson's trichrome was used to analyze the extent of fibrotic tissues. Rabbit anti-TNAP (Abcam, 1:200), anti-α-SMA (Abcam, 1:300) and anti-vimentin (Abcam, 1:300) antibodies were used as primary antibodies for immunochemical staining overnight at 4 °C, followed by incubations with secondary antibodies and DAB reagents. The quantitative analysis of the fibrotic area and TNAP, vimentin and α-SMA expression in heart tissues was performed using Image-Pro-Plus 6.0 software.

2.7. Cell isolation and culture

Cardiac fibroblasts (CFs) were isolated from neonatal (1−3 days) C57BL/6 J mice and identified by vimentin expression. Left ventricles were dissected from the mouse heart, finely minced into pieces, and then digested with 0.25% trypsin/EDTA (Beyotime Biotechnology, Shanghai, China) and Collagenase II (Bopei Biotech Co. Ltd, Chongqing, China) at 37 °C. Subsequently, the suspensions of CFs were centrifuged, resuspended, plated, and incubated for 1.5 h. Then, the suspensions of CFs were cultured on soft plates (Advanced Biomatrix, CytoSoft®, Elastic Moduli 8 kPa) coated with laminin (0.5 μg/cm^2, BioLamina). Adherent cells expressing vimentin were isolated as CFs, and passages 1 cells were used for our experiments. CFs were maintained in DMEM supplemented with 10% fetal bovine serum (Wisent, Canada) and 100 U/ml penicillin and streptomycin and incubated at 37 °C in a humidified chamber.

2.8. Cardiac fibroblast transfection with adenoviruses

CFs were plated at approximately 60% confluence and transfected with adv-shTNAP, adv-TNAP-OE or the appropriate control according to the manufacturer's instructions. Forty-eight hours after transfection, hypoxia (37 °C, 5% CO_2 and 1% O_2) was applied to CFs for 24 h, and then the cells were harvested for further analysis. For stimulation with recombinant human transforming growth factor-β1 (TGF-β1, R&D Systems, Inc, USA), 24 h after transfection, cells were exposed to serum-free medium for 24 h. After starvation, TGF-β1 protein (10 ng/ml) was applied to CFs for another 24 h.

2.9. Western blot analysis

RIPA buffer containing phenylmethylsulfonyl fluoride (PMSF, Beyotime) and protein phosphatase inhibitor was used to lyse frozen mouse heart tissues and CFs. Lysates were centrifuged at 12,000 rpm for 10 min to remove all cell debris, and the protein concentration in the supernatant was assayed using a BCA Protein Assay Kit (Beyotime Biotechnology, Shanghai, China). Loading dye (Beyotime Biotechnology) was added to the samples before heating at 100°C for 15 mins. Total proteins were separated by SDS-PAGE on a 10% gel and then transferred onto polyvinylidene difluoride (PVDF) membranes. Membranes were incubated with the following primary antibodies: TNAP (Abcam, 1:1000), Collagen I (Abcam, 1:1000), α-SMA (Abcam, 1:1000), TGF-β1 (Sigma-Aldrich, 1:1000), p-Smad2 (Cell Signaling Technology, 1:1000), Smad2 (Cell Signaling Technology, 1:1000), p-Smad3 (Cell Signaling Technology, 1:1000), Smad3 (Cell Signaling Technology, 1:1000), p-ERK1/2 (Cell Signaling Technology, 1:1000), ERK1/2 (Cell Signaling Technology, 1:1000), Cyclin D1 (Abcam, 1:5000), CDK2 (Abcam, 1:1000), GAPDH (ImmunoWay, 1:5000) and Cyclin E1 (ImmunoWay Biotechnology, 1:1000). Next, membranes were incubated with horseradish peroxidase (HRP)-conjugated secondary antibodies (1:5000, Santa Cruz, USA). The bands were visualized using Immobilon Western HRP (Millipore, Germany). RRID tags for all antibodies are shown in **Supplementary Table 2**. All antibodies were validated by manufacturers.

2.10. Immunofluorescence staining of CFs

CFs (1.5×105 cells/ml) were seeded in 24-well plates after transfection with adv-shTNAP, adv-TNAP-OE or the negative plasmid, and stimulation with TGF-β1 (10 ng/ml). Then, the cells were permeabilized with 0.1% Triton X-100 for 20 min, blocked with 10% goat serum in PBS-Tween for 1 h at room temperature, and incubated with the α-SMA and vimentin antibody at 4 °C overnight. CFs were incubated with a FITC-conjugated secondary antibody (1:100; Proteintech Group, Inc, Wuhan, China) for 1 h. Finally, DAPI was used to counterstain nuclei. The results were measured using confocal laser scanning microscopy.

2.11. Wound healing and cell proliferation assay

The migration capability of cells was evaluated by performing a wound healing assay. CFs were seeded in 6-well plates at 70% confluence. After transfection with adenoviruses, the cells were scratched with a sterile 200 μl micropipette tip followed by two gentle rinses with PBS and an incubation under hypoxic conditions for 24 h. Images were captured at 0 and 24 h after scratching. ImageJ software was used to measure the migration distances. Cell proliferation was evaluated utilizing a CCK-8 kit (MedChemExpress, Monmouth Junction, NJ) according to the manufacturer's instructions. The absorbance of each well was measured at 450 nm using a microplate reader (Multiskan MK33, Thermolab Systems, Helsinki, Finland).

2.12. Flow cytometry analyses

Flow cytometry samples were prepared 48 h after cells were transfected with adenoviruses. CFs were digested with trypsin, centrifuged (1000 rpm $\times$ 5 min), washed (cold PBS), collected, and fixed with 70% cold ethanol at 4 °C overnight. After removing the fixation solution, cell samples were incubated at 37 °C with the propidium iodide (PI) working solution containing 10 ml of RNase A for 30 min. A FACScan flow cytometer (CytoFLEX) was used to analyze the cell samples at excitation/emission wavelengths of 488/575 nm. Each sample was analysed three times and at least three independent experiments were performed.

2.13. Quantitative real-time PCR

Total RNA was extracted from heart tissues or CFs using TRIzol reagent (Invitrogen) and was converted to cDNAs using the QuantiTect Reverse Transcription Kit (Qiagen Co., Germany) according to the manufacturer's protocol. All results were quantified using the comparative CT method. The PCR primers were obtained from Sangon Biotech, Co. (Shanghai, China), and primer sequences are listed in **Supplemental Table 3**.

2.14. Ethics statement

The correlation analysis conformed to the STROBE guidelines for observational cohort and case-control studies. A STROBE guideline checklist is included in **Supplementary Checklist 1**. All patients provided written informed consent before participation in the study. The protocol for animal experiments was carried out in accordance with institutional animal welfare guidelines and followed the ARRIVE guidelines for reporting animal research. An ARRIVE guideline checklist is included in **Supplementary Checklist 2**. All studies were reviewed and approved by the ethics committee of Chongqing Medical University (Number 2017−174) and conformed to the principles outlined in the Declaration of Helsinki.

2.15. Statistical analysis

For the systematic review and meta-analysis, dichotomous data were analysed by calculating relative risks (RRs) with 95% confidence intervals (CIs). The presence of significant heterogeneity was assessed using the Q-statistic, and the extent of the observed heterogeneity was assessed using the I^2 statistic. Pooled analyses were calculated using random-effect models. We visually examined funnel plots for primary endpoints and further assessed asymmetry using the Begg and Egger tests to detect any publication bias. Statistical analyses were performed using the RevMan software package (Review Manager, version 5.3).

Continuous data are presented as the means and standard errors of the means (SEM) if they were normally distributed or medians (interquartile ranges: [IQRs)] if they were not normally distributed. The association between serum TNAP levels and fibrosis biomarkers was assessed using Pearson's correlation analysis. Student's t-test was used for comparisons between two groups. One-way ANOVA followed by Tukey comparison test was used for comparison between at least three groups. The Kaplan−Meier product-limit estimation method was used to estimate the survival rates of mice, and the statistical differences were compared using log-rank tests. A value of $P < 0.05$ was considered significant. All data were analysed using SPSS (version 22.0) statistical software.

2.16. Role of funding source

This study was supported by the National Natural Science Foundation of China, 81,970,203; National Natural Science Foundation of China, 31,800,976; and Chongqing Science and Health Joint Medical Research Project, 2018QNXM024 and Natural Science Foundation of Chongqing, cstc2018jcyjA0153. Funders did not have any role in the study design, data collection, data analysis, interpretation, or writing of the manuscript.

3. Results

3.1. Increased TNAP levels are associated with fibrosis level of patients with myocardial infarction

A flow diagram of the study selection process is shown in **Supplemental Fig. 1.** After searching the main databases and performing a detailed assessment of the full-text articles, eight studies with 14,816 individuals were included in the quantitative analysis. The baseline characteristics of the included studies are summarized in **Supplemental Table 4.** According to the meta-analysis, a high serum TNAP level was associated with an increased risk of all-cause mortality (RR: 1.89; 95% CI, 1.48 to 2.42; $P<0.001$, Fig. 1**a**) and cardiovascular mortality (RR: 1.85; 95% CI, 1.33 to 2.59; $P<0.001$, Fig. 1**b**) in patients with IHD. TNAP levels were also associated with an increased risk of all-cause mortality in patients with MI (RR: 1.71; 95% CI, 1.36 to 2.16; $P<0.001$, Fig. 1**c**). In different subgroups, serum TNAP levels were still associated with an increased risk of all-cause mortality (Fig. 1**d**). A visual inspection of funnel plots of all studies showed symmetry, indicating a low risk of publication bias (P_{Begg}=0.17 and P_{Egger}=0.40, Fig. 1**e**).

TNAP expression was upregulated in the heart tissue of patients with MI. Heart tissues were obtained from donors who died from MI. The baseline characteristics of the 5 patients are summarized in **Supplemental Table 5**. The left ventricular tissues displayed abundant deposition of collagen with Masson's trichrome staining (Fig. 2**a**). Immunohistochemistry results showed that heart tissues with MI exhibited significantly increased expression of TNAP and α-SMA, and the distribution of TNAP was consistent with the distribution of α-SMA and collagen, which suggested a potential correlation between TNAP expression and cardiac fibrosis after MI.

Next, we measured the serum PICP, PIIINP and TNAP levels in 31 patients with MI and 28 patients without coronary artery disease (CAD). The baseline characteristics of the included patients are described in **Supplemental Table 6**. The concentrations of TNAP, PICP and PIIINP in patients with MI were significantly higher than those in patients without CAD (Fig. 2**b-d**). The TNAP level was significantly positively correlated with the concentrations of PICP and PIIINP (Fig. 2**e-f**). All these results indicated a strong relationship between increased TNAP expression and cardiac fibrosis in humans with MI.

3.2. TNAP expression is upregulated in mice after MI surgery

Mouse models of MI were established to represent the aforementioned cardiac fibrotic responses and investigate whether TNAP

a

Study or Subgroup	High TNAP Events	Total	Low TNAP Events	Total	Weight	Risk Ratio M-H, Random, 95% CI	Year
Tonelli et al	155	1374	87	1349	17.4%	1.75 [1.36, 2.25]	2009
Park et al	70	532	17	541	11.0%	4.19 [2.50, 7.02]	2013
Nunes et al	30	72	31	123	13.4%	1.65 [1.10, 2.49]	2016
Kim et al	78	433	63	444	16.1%	1.27 [0.94, 1.72]	2017
Ndrepepa et al	196	1846	117	1855	18.2%	1.68 [1.35, 2.10]	2017
Yu et al	30	2122	10	2123	7.7%	3.00 [1.47, 6.12]	2019
Gao et al	8	201	6	625	4.4%	4.15 [1.46, 11.81]	2020
Oh et al	37	590	27	586	11.7%	1.36 [0.84, 2.21]	2020
Total (95% CI)		**7170**		**7646**	**100.0%**	**1.89 [1.48, 2.42]**	
Total events	604		358				

Heterogeneity: Tau² = 0.07; Chi² = 21.42, df = 7 (P = 0.003); I² = 67%
Test for overall effect: Z = 5.08 (P < 0.00001)

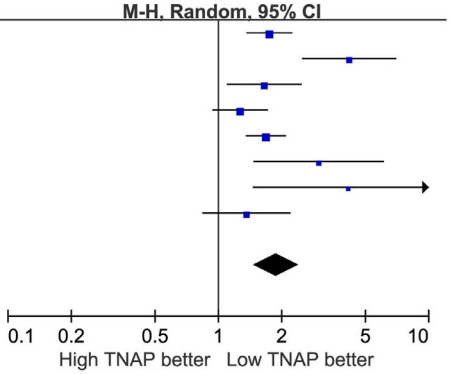

b

Study or Subgroup	High TNAP Events	Total	Low TNAP Events	Total	Weight	Risk Ratio M-H, Random, 95% CI	Year
Tonelli et al	79	1374	56	1349	26.7%	1.39 [0.99, 1.93]	2009
Park et al	35	532	10	541	14.2%	3.56 [1.78, 7.11]	2013
Ndrepepa et al	130	1846	71	1855	29.0%	1.84 [1.39, 2.44]	2017
Kim et al	41	433	32	444	22.2%	1.31 [0.84, 2.05]	2017
Gao et al	8	201	6	625	7.9%	4.15 [1.46, 11.81]	2020
Total (95% CI)		**4386**		**4814**	**100.0%**	**1.85 [1.33, 2.59]**	
Total events	293		175				

Heterogeneity: Tau² = 0.08; Chi² = 10.22, df = 4 (P = 0.04); I² = 61%
Test for overall effect: Z = 3.63 (P = 0.0003)

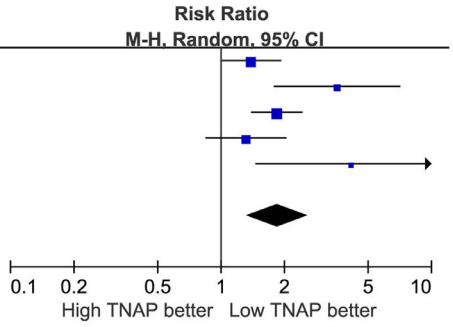

c

Study or Subgroup	High TNAP Events	Total	Low TNAP Events	Total	Weight	Risk Ratio M-H, Random, 95% CI	Year
Tonelli et al	155	1374	87	1349	50.5%	1.75 [1.36, 2.25]	2009
Nunes et al	30	72	31	123	25.4%	1.65 [1.10, 2.49]	2016
Gao et al	8	201	6	625	4.7%	4.15 [1.46, 11.81]	2020
Oh et al	37	590	27	586	19.4%	1.36 [0.84, 2.21]	2020
Total (95% CI)		**2237**		**2683**	**100.0%**	**1.71 [1.36, 2.16]**	
Total events	230		151				

Heterogeneity: Tau² = 0.01; Chi² = 3.67, df = 3 (P = 0.30); I² = 18%
Test for overall effect: Z = 4.55 (P < 0.00001)

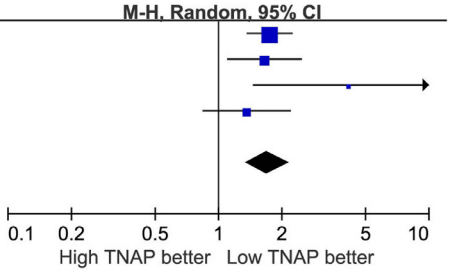

d

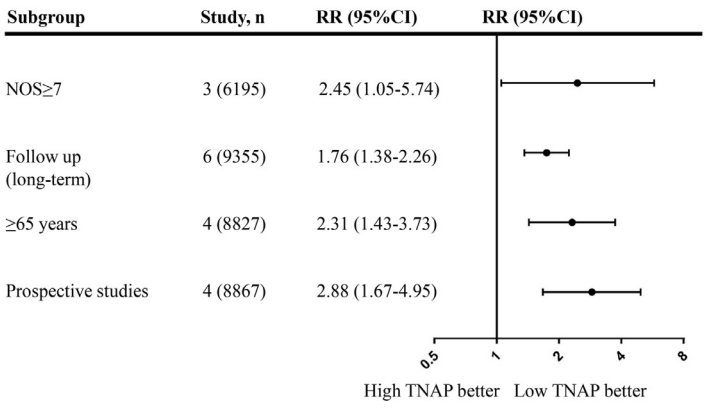

e

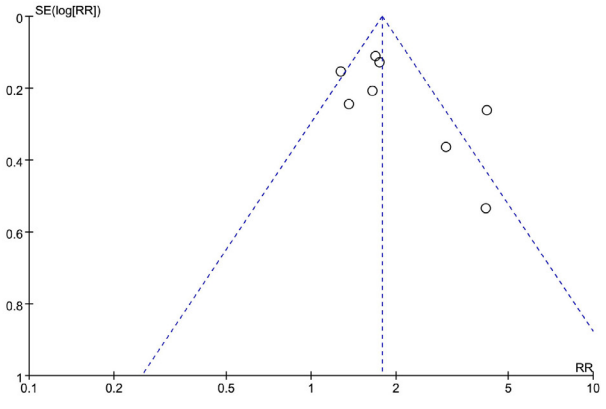

Fig. 1. Meta-analysis of the effect of serum TNAP levels on mortality in patients with IHD. (**a**) The effect of serum TNAP levels on all-cause mortality in patients with IHD. (**b**) The effect of serum TNAP levels on cardiovascular mortality in patients with IHD. (**c**) The effect of serum TNAP levels on all-cause mortality in patients with MI. (**d**) Subgroup analysis according to characteristics of the include studies. (**e**) Funnel plots for the endpoint of all-cause mortality in patients with IHD. Meta-analyses were calculated using random-effect models.

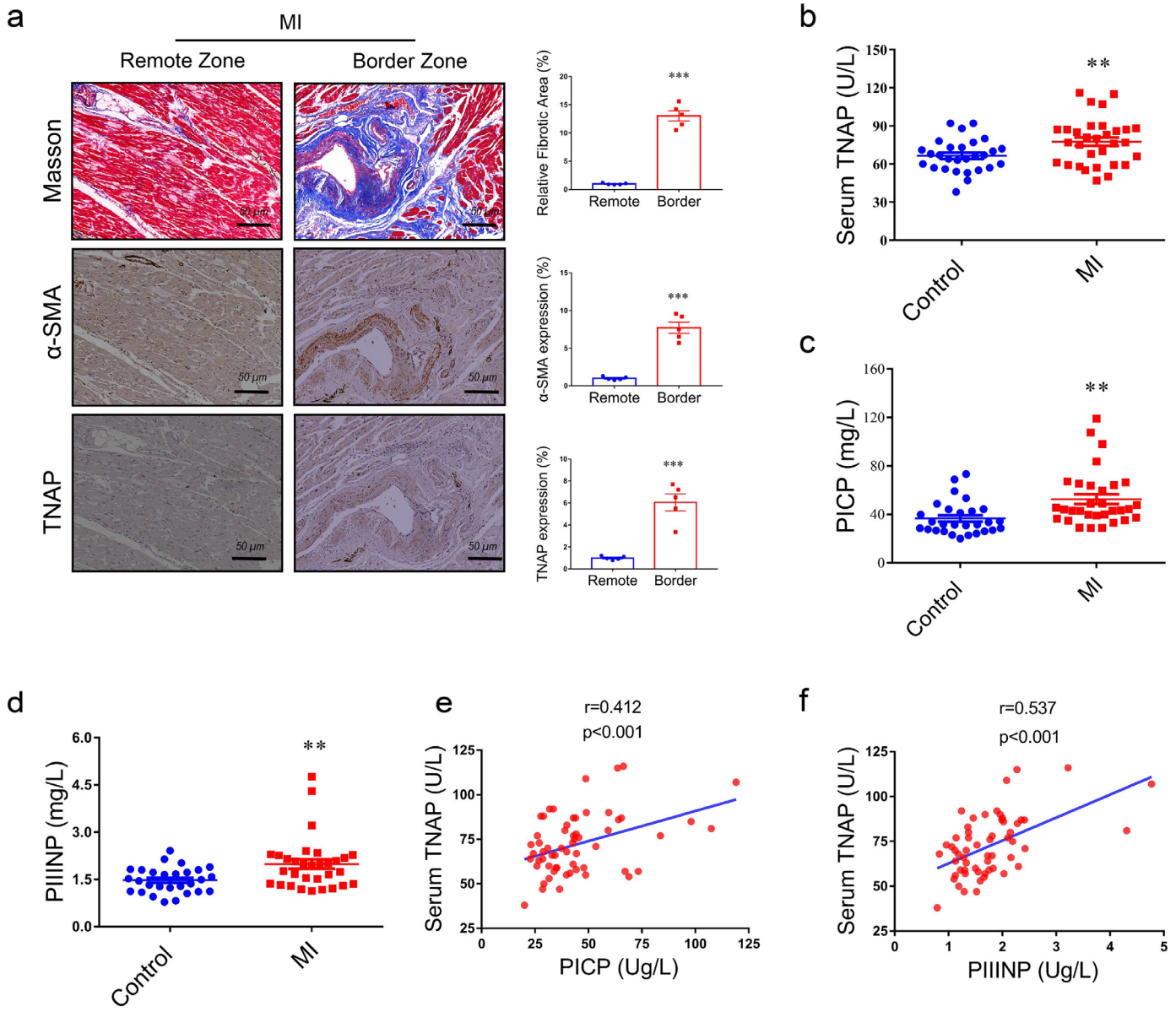

Fig. 2. Increased TNAP is associated with cardiac fibrosis in patients with myocardial infarction. (**a**) Representative images of Masson's trichrome staining and immunohistochemical staining of α-SMA and TNAP in the left ventricle from patient with MI. n = 4 per group, scale bar represents 50 μm. (**b**) The concentration of serum TNAP in patients with MI. (**c**) The concentration of serum PICP in patients with MI. (**d**) The concentration of serum PIIINP in patients with MI. (**e**) Correlation analysis between serum TNAP level and PICP concentration. (**f**) Correlation analysis between serum TNAP level and PIIINP concentration. Continuous data were expressed as mean ± SEM. To-tailed unpaired Student's t-test was used to test the difference. $^{*}P < 0.05$. $^{**}P<0.01$, $^{***}P<0.001$.

expression is related to cardiac fibrosis in mice. The distribution of TNAP was also consistent with the distribution of collagen, as evidenced by Masson's trichrome and immunohistochemistry (Fig. 3**a**). Western blot analysis indicated that TNAP expression peaked within 14 days after MI surgery and then was maintained at parallel levels to the activated myofibroblast marker α-SMA and collagen I deposition (**Supplemental Fig. 2**).

3.3. Knockdown of TNAP ameliorates cardiac fibrosis and improves cardiac function in vivo

We generated adenovirus-mediated TNAP knockdown and negative plasmids (adv-scramble) to clarify the role of TNAP in cardiac fibrosis following MI. The procedure for injecting mice with adenovirus is shown in Fig. 3**b**. As expected, MI mice injected with the adv-scramble exhibited a significantly reduced LVEF and FS and enlarged LVIDs and LVIDd compared with mice that underwent the sham procedure (Fig. 3**c**). MI mice injected with the adv-shTNAP exhibited a significant improvement in LVEF, FS, LVIDd and LVIDs compared with those injected with adv-scramble 14 days after MI surgery. Additionally, TNAP knockdown was associated with a trend toward decreasing the risk of death after MI (Fig. 3**d**).

TNAP knockdown reduced the infarct area of the left ventricle and overall collagen deposition, as shown by Masson's trichrome staining (Fig. 3**e**). Compared with the sham group, the concomitant expression of vimentin and α-SMA was significantly upregulated in the MI mice injected with the adv-scramble (Fig. 3**e**). However, MI mice injected with adv-shTNAP exhibited a significant reduction in the expression of vimentin and α-SMA compared with those injected with adv-scramble. Western blot analysis indicated significantly reduced TNAP expression in the mouse heart injected with adv-shTNAP (Fig. 3**f**). The MI-induced expression of the Collagen I and α-SMA proteins was significantly attenuated by the injection of adv-shTNAP, suggesting that TNAP knockdown inhibited the activation of cardiac

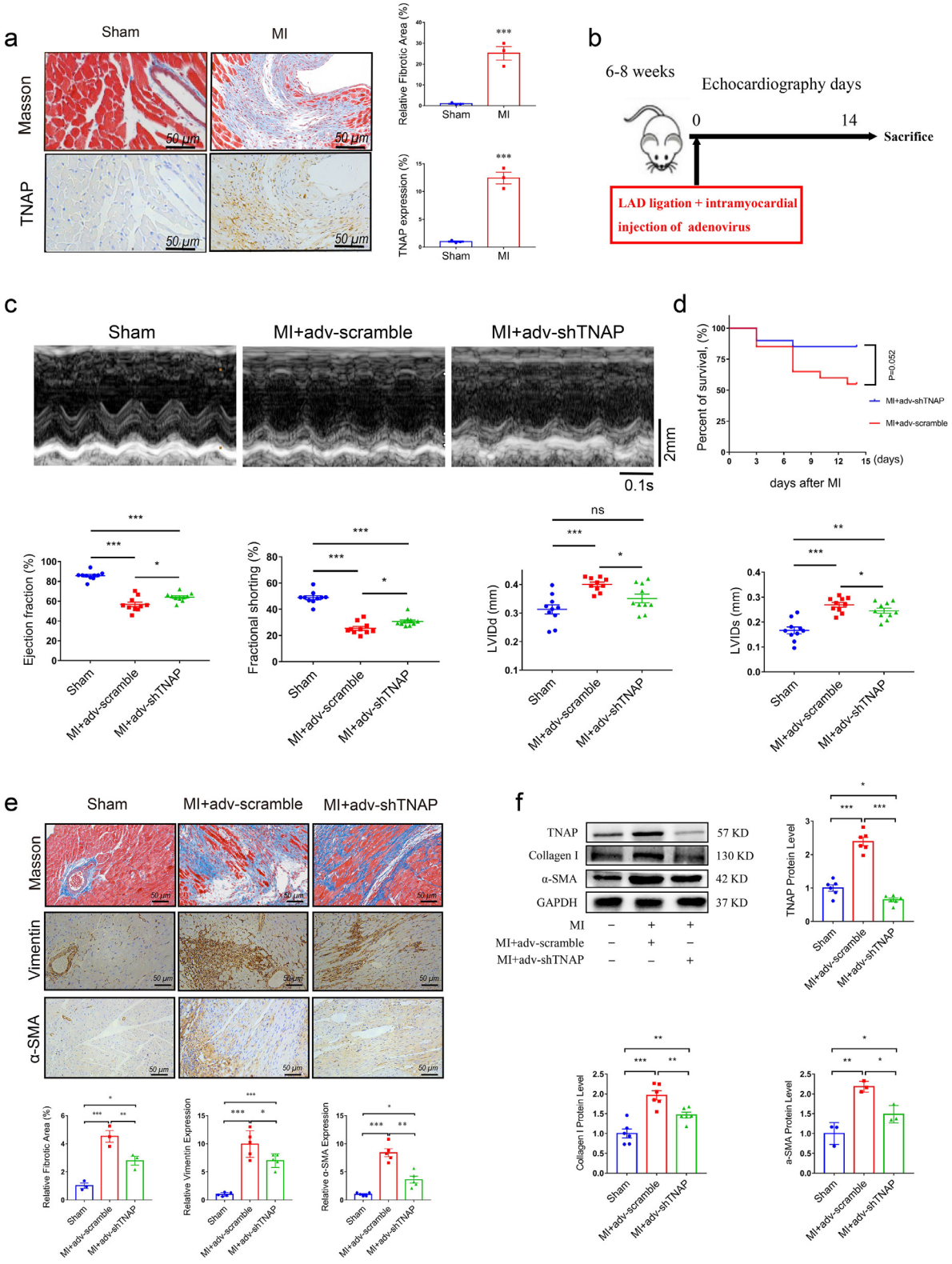

Fig. 3. TNAP knockdown improves cardiac function and ameliorates cardiac fibrosis after MI surgery in vivo. (**a**) Representative images of Masson's trichrome staining and immunohistochemical staining of TNAP in the left ventricle from a sham heart and from an infarcted heart at 14 days after MI surgery. n = 4 mice per group, scale bar represents 50 μm. (**b**) Procedure for mice injecting with adenovirus. (**c**) M-mode images of mice injected with or without adv-shTNAP at 14 days after MI surgery, n = 10 mice per group. Time stamp in seconds at the bottom, scale bar in mm on the right. (**d**) Kaplan-Meier survival curves of mice injected with adv-scramble and adv-shTNAP after MI surgery. (**e**) Images of Masson's trichrome staining and immunohistochemical staining of vimentin and α-SMA in transverse sections from an infarcted heart injection with adv-shTNAP at the 14 days after MI surgery. n = 5 mice per group. (**f**) TNAP (n = 6 mice per group), Collagen I (n = 6 mice per group) and α-SMA (n = 3 mice per group) expressions in heart tissues of mice were assessed by western blot. Data were expressed as mean ± SEM. Two-tailed unpaired Student's t-test (a) or 1-way ANOVA test (c, e-f) was used to test the difference. $^{*}P<0.05$, $^{**}P<0.01$, $^{***}P<0.001$.

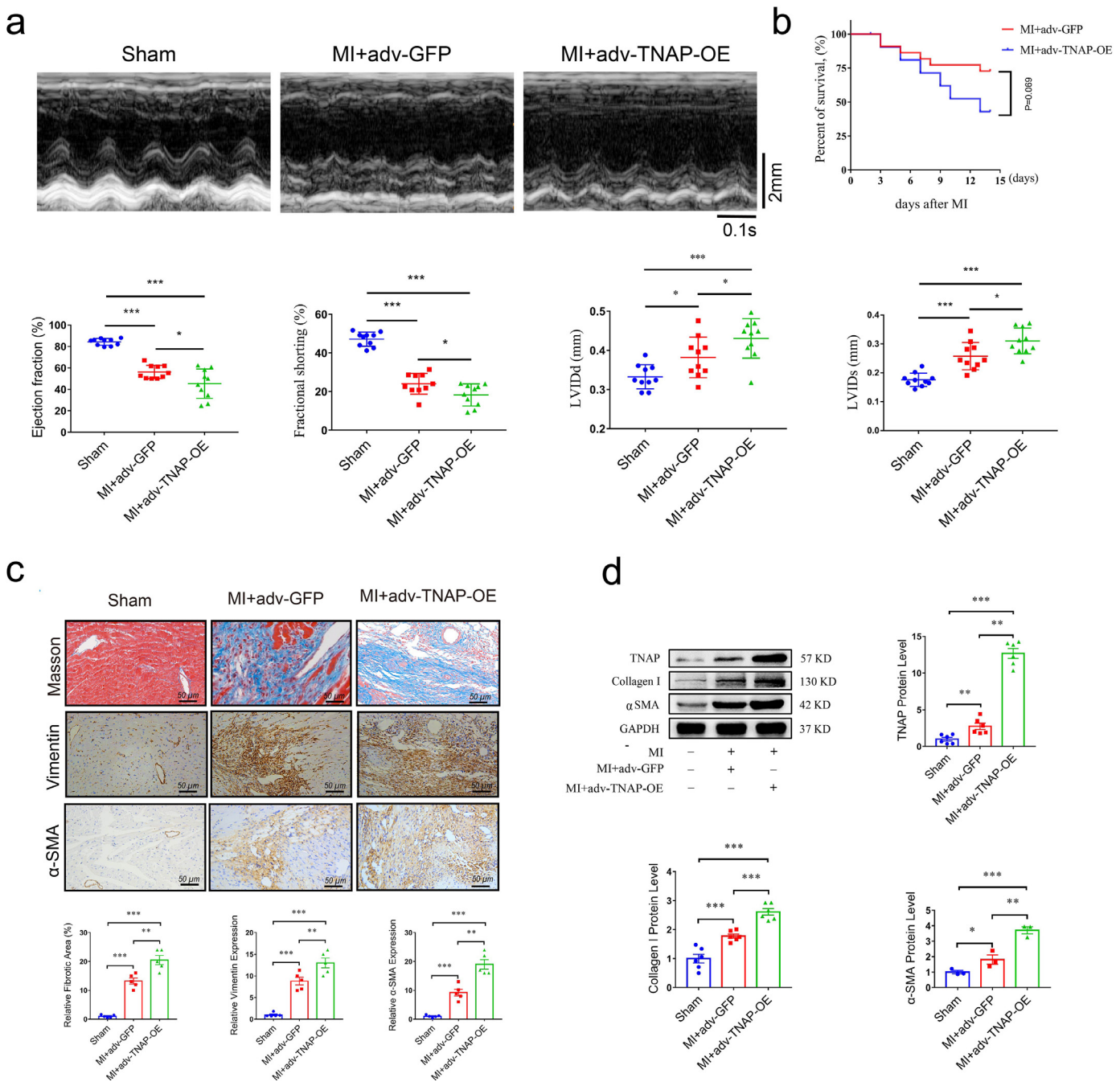

Fig. 4. TNAP overexpression worsens cardiac function and aggravates cardiac fibrosis after MI surgery in vivo. (**a**) M-mode images of mice injected with or without adv-TNAP-OE at 14 days after MI surgery. n = 10 mice per group. Time stamp in seconds at the bottom, scale bar in mm on the right. (**b**) Kaplan-Meier survival curves of mice injected with adv-GFP and adv-TNAP-OE at 14days after MI surgery. (**c**) Images of Masson's trichrome staining and immunohistochemical staining of vimentin and α-SMA in transverse sections from an infarcted heart injection with adv-TNAP-OE at the 14 days after MI surgery. n = 5 mice per group. (**d**) TNAP (n = 6 mice per group), Collagen I (n = 6 mice per group) and α-SMA (n = 3 mice per group) expressions in heart tissues of mice were assessed by western blot and quantified according to the immunoblots. Data were expressed as mean ± SEM. One-way ANOVA test (a, c, d) was used to test the difference. $^{*}P<0.05$, $^{**}P<0.01$, $^{**}P<0.001$.

myofibroblasts in vivo. Altogether, these findings suggested that TNAP knockdown improved cardiac function and ameliorated cardiac fibrosis after MI surgery.

3.4. *Overexpression of TNAP aggravates cardiac fibrosis and worsens cardiac function in vivo*

We generated adenovirus-mediated TNAP overexpression (adv-TNAP-OE) and negative control plasmids (adv-GFP) to elucidate the role of TNAP overexpression in cardiac fibrosis following MI surgery. In contrast to the findings obtained with TNAP knockdown, MI mice injected with adv-TNAP-OE exhibited a dramatic reduction in EF and FS, and enlarged LVIDd and LVIDs compared with those injected with adv-GFP (Fig. 4**a**). Additionally, although no significant difference was observed, TNAP overexpression exhibited a trend towards increasing the risk of death after MI surgery (Fig. 4**b**).

Masson's trichrome staining showed that TNAP overexpression aggravated the infarcted area of the left ventricle and overall collagen deposition (Fig. 4**c**). Immunochemistry showed that MI mice injected with adv-TNAP-OE exhibited dramatically upregulated expression of vimentin and α-SMA compared with those injected with adv-GFP (Fig. 4**c**). The expression of the TNAP protein was significantly

upregulated by the adv-TNAP-OE injection. Dramatically increased expression of α-SMA and Collagen I was observed in mice injected with adv-TNAP-OE (Fig. 4**d**), suggesting that TNAP overexpression promoted the activation of cardiac myofibroblasts in vivo. Based on these findings, TNAP overexpression aggravated cardiac fibrosis and worsened cardiac function in vivo after MI.

3.5. TNAP regulates cardiac fibroblast differentiation, migration and proliferation in vitro

Cardiac fibroblasts (CFs) isolated from neonatal C57BL/6 J mice (1−3 days) were identified by vimentin expression (**Supplemental Fig. 3**). We investigated the expression of TNAP, Collagen I and TGF-β1 in CFs at different time points after hypoxia induction (37 °C, 5% CO_2 and 1% O_2) to explore optimal hypoxia time points for subsequent experiments. Western blot analysis showed increased expression of TNAP with a prolonged hypoxia time, and the difference was significant at 24 h, similar to changes in the expression of α-SMA and collagen I (**Supplemental Fig. 4**).

CFs were infected with adv-shTNAP followed by incubation under hypoxic conditions for 24 h to determine whether TNAP knockdown attenuated the hypoxia-induced activation of CFs. The efficiency of TNAP knockdown in vitro was assessed by performing western blot and RT-PCR assays. The expression of the TNAP protein and mRNA in CFs was effectively blocked by adv-shTNAP transfection (**Supplemental Fig. 5a**). Hypoxia induced a remarkable increase in Collagen I expression compared with the adv-scramble group. Similar to the findings of the in vivo study, TNAP knockdown markedly inhibited α-SMA and Collagen I expression (Fig. 5**a**), suggesting that TNAP knockdown inhibited hypoxia-induced CF differentiation. CFs migration was measured using wound healing assays. Hypoxia significantly induced CFs migration compared to normoxia group, and TNAP knockdown dramatically inhibited hypoxia-induced CFs migration (Fig. 5**b**). The proliferation of CFs is another essential factor contributing to the pathogenesis of cardiac fibrosis [18]. The effect of TNAP knockdown on CFs proliferation was measured using CCK-8 assay. As shown in Fig. 5**c**, TGF-β1 stimulated the proliferation of CFs, while TNAP knockdown significantly reduced the growth rate of CFs.

The expression of the TNAP protein and mRNA in CFs was effectively increased by adv-TNAP-OE transfection (**Supplemental Fig. 5b**). In contrast to the findings obtained from cells with TNAP knockdown, TNAP overexpression significantly increased α-SMA and Collagen I expression (Fig. 5**d**), suggesting that TNAP overexpression promoted hypoxia-induced myofibroblast activation. In addition, TNAP overexpression significantly enhanced hypoxia-induced CFs migration (Fig. 5**e**). As shown in Fig. 4**f**, TNAP overexpression significantly accelerated the growth rate of CFs.

3.6. TNAP functions through the TGF-β1/Smads and ERK1/2 signaling pathways

TGF-β/Smads are the main mediators of cardiac fibrosis after MI [19]. In vivo studies confirmed that mouse hearts exhibited a greater TGF-β1 expression and Smad2/3 phosphorylation after MI. TNAP knockdown suppressed these increases (Fig. 6**a**), while TNAP overexpression enhanced them (Fig. 6**b**). Several studies have proposed that ERK1/2 activation is required for the proliferation of CFs [20−22]. The levels of phosphorylated ERK1/2 in the adv-TNAP-OE MI group were higher than those in the adv-GFP MI group, but the increase was significantly attenuated by the injection of adv-shTNAP after MI (Fig. 6**a-b**). Thus, TGF-β1/Smads and ERK1/2 signaling may mediate the effect of TNAP on cardiac fibrosis after MI.

For further verification, CFs were cultured and transfected with the adenovirus as described above. Hypoxia induced the expression of TGF-β1 and the phosphorylation of Smad2/3 in CFs. Western blotting showed that TNAP knockdown dramatically limited the conversion of hypoxia-induced fibroblasts into myofibroblasts, accompanied by the suppression of TGF-β1 expression and phosphorylation of Smad2/3 (Fig. 6**c**). In contrast, TNAP overexpression increased the expression of TGF-β1 and the phosphorylation of Smad2/3 induced by hypoxia (Fig. 6**d**). TNAP knockdown markedly attenuated the level of phosphorylated ERK1/2 induced by TGF-β1 (Fig. 6**e**), while TNAP overexpression increased the level of phosphorylated ERK1/2 (Fig. 6**f**). These findings indicated that TGF-β1/Smads and ERK1/2 signaling were involved in the pro-fibrotic effect of TNAP on CFs.

To future explore the mechanism by which TNAP promotes CFs growth, we performed flow cytometry to quantify the cell cycle distribution and observed an increased number of adv-shTNAP-transfected CFs in G0/G1 phase and reduced number in S phase (Fig. 7**a**), but no significant change was observed in the number of cells in G2/M phase, indicating that TNAP knockdown may induce cell cycle arrest at the G1/S transition. TNAP knockdown also suppressed the TGF-β1-induced expression of cyclin E1, cyclin D1 and CDK2 (Fig. 7**b**). In contrast, the opposite flow cytometry results were obtained from adv-TNAP-OE-transfected CFs. The number of cells was reduced in G0/G1 phase and increased in S phase after CFs were transfected with adv-TNAP-OE (Fig. 7**c**). TNAP overexpression did not exert a significant effect on the distribution of cells in G2/M phase. Additionally, TNAP overexpression upregulated the TGF-β1-induced expression of cyclin E1, cyclin D1 and CDK2 in CFs (Fig. 7**d**).

CFs transfected with adv-TNAP-OE were incubated with TGF-β1 and U0126 (10 μmol/L, a specific inhibitor of ERK1/2) for 24 h before harvest to further clarify the role of the ERK1/2 signaling pathway [20]. Western blotting showed that U0126 inhibited the expression of the α-SMA and Collagen I proteins in adv-TNAP-OE-transfected CFs (Fig. 8**a**). The proliferation of CFs induced by TNAP overexpression was effectively blocked by U0126 (Fig. 8**b**). Immunofluorescence staining showed that U0126 inhibited the expression of the vimentin and α-SMA proteins in adv-TNAP-OE-transfected CFs (Fig. 8**c**). Collectively, TNAP regulated CF differentiation, migration and proliferation by activating the TGF-β1/Smads and ERK1/2 signaling pathways.

4. Discussion

Based on our data, high serum TNAP levels were associated with an increased risk of mortality in patients with IHD and MI. The distribution of TNAP is consistent with the area of α-SMA and collagen deposition in the hearts of both humans and mice with MI. Serum TNAP levels is positively correlated with fibrosis biomarker concentrations in patients with MI. In vitro studies showed that TNAP promoted collagen deposition and aggravated cardiac function in mice after MI. In contrast, TNAP knockdown alleviated cardiac fibrosis and improved cardiac function. Mechanistically, TNAP activated the TGF-β1/Smads and ERK1/2 signaling pathways, both of which propelled the fibrotic process after MI. Additionally, TNAP promoted the proliferation of CFs by increasing the number of cells transitioning from G1 phase to S phase.

Several clinical studies have investigated the relationship between serum TNAP levels and mortality in IHD [7,8,23,24]. Our previous small-sample study found that serum TNAP levels may be associated with an increased risk of in-hospital mortality [12]. In the present study, we perform a pooled analysis of over 14, 000 patients and found that TNAP levels were associated with increased risks of both all-cause and cardiovascular mortality, consistent with the results of the CARE study [7]. Interestingly, the results of the CARE study also reported that high serum TNAP levels significantly increased the risk of heart failure in patients with MI. Cardiac fibrosis plays a crucial role in ventricular remodeling, heart failure and cardiovascular mortality [2,3,25]. Serum PICP and PIIINP levels have been confirmed to be associated with the extent of collagen type I and type III deposition, respectively [17,26]. Here, the serum TNAP

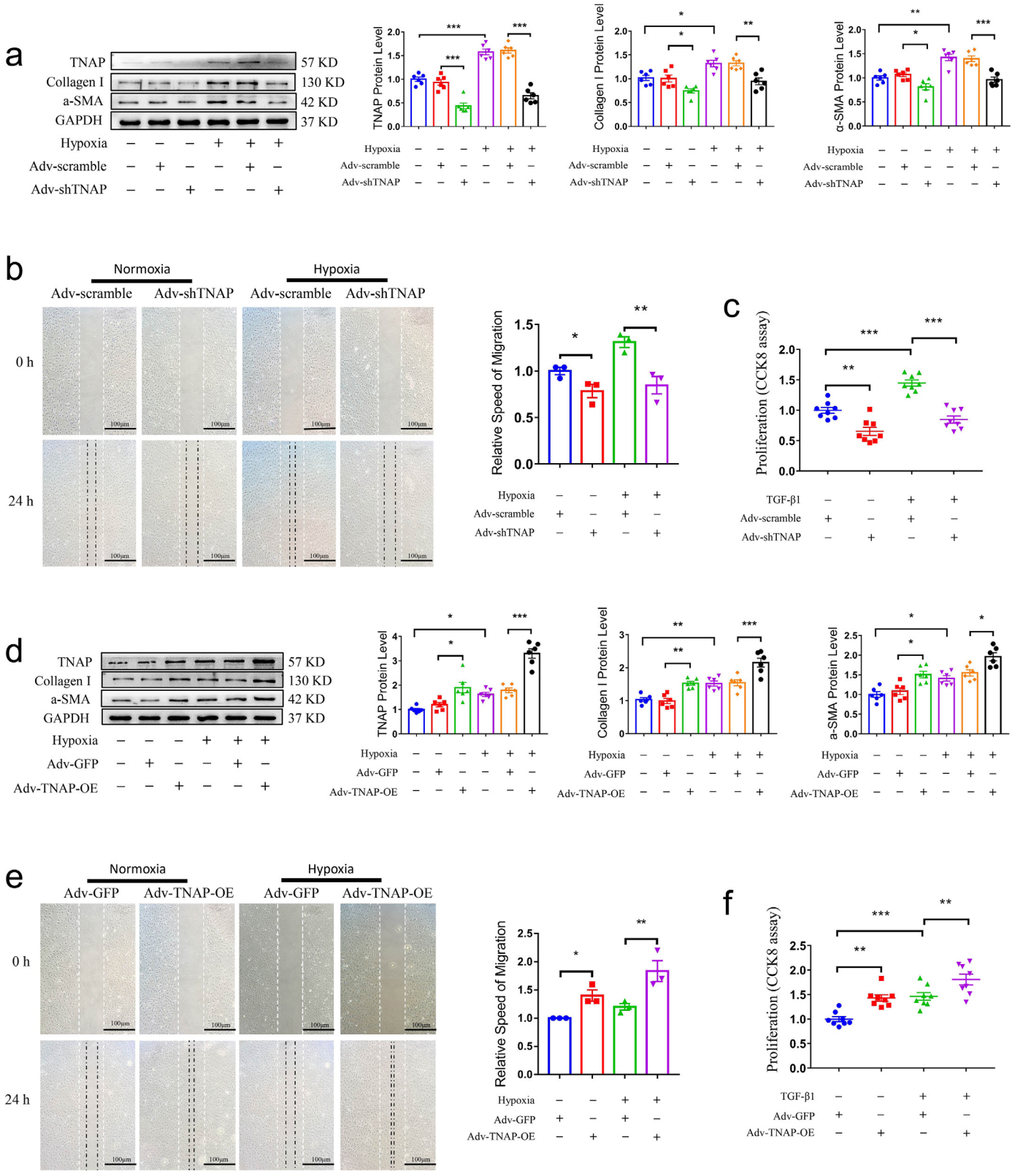

Fig. 5. TNAP regulated cardiac fibroblasts (CFs) differentiation, migration and proliferation in vitro. (**a**) Cultured CFs transfected with adv-scramble or adv-shTNAP and incubated with hypoxia for 24 h, the protein levels of TNAP, α-SMA and Collagen I in were measured by western blot and quantified by immunoblots. n = 6 per group. (**b**) Images of scratch assay of CFs transfected with adv-scramble or adv-shTNAP and incubated with or without hypoxia for 24 h. n = 3 per group. (**c**) CCK-8 proliferation assay of CFs transfected with or without adv-shTNAP and incubated with TGF-β1 (10 ng/ml) for 24 h. n = 8 per group. (**d**) The protein levels of TNAP, α-SMA and collagen I in cultured CFs transfected with adv-GFP or adv-TNAP-OE were assessed by western blot. n = 6 per group. (**e**) Images of scratch assay of CFs transfected with adv-GFP or adv-TNAP-OE and incubated with or without hypoxia for 24 h. n = 3 per group. (**f**) CCK-8 proliferation assay of primary CFs transfected with or without adv-TNAP-OE and incubated with TGF-β1 for 24 h. n = 8 per group. Data were expressed as mean ± SEM. One-way ANOVA test was used to test the difference. $^{*}P<0.05$, $^{**}P<0.01$, $^{***}P<0.001$.

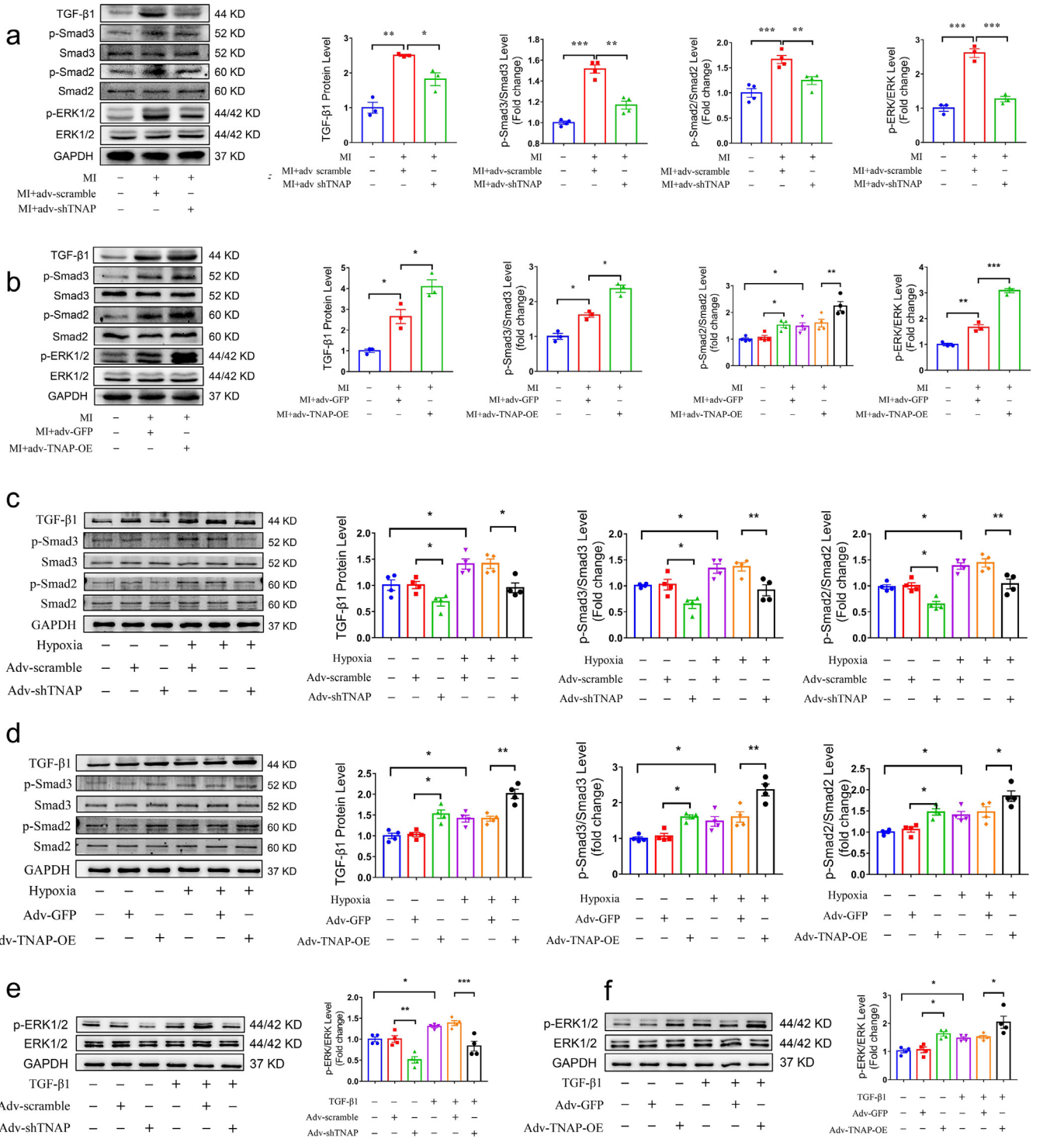

Fig. 6. TNAP promotes CFs activation by regulating TGF-β1/Smads and ERK1/2 signaling pathways. (**a**) Inhibition of TGF-β/Smads and ERK1/2 signaling in vivo in a mouse model of MI following adv-shTNAP injection was detected and quantified via western blot. n = 3–4 per group. (**b**) Activation of TGF-β/Smads and ERK1/2 signaling vivo in a mouse model of MI following adv-TNAP-OE injection was detected and quantified via western blot. n = 3–4 per group. (**c**) TGF-β/Smads signaling in cultured CFs transfected with adv-shTNAP for 48 h and exposed to hypoxia for 24 h, the results were measure by western blot. n = 4 per group. (**d**) TGF-β/Smads signaling in cultured CFs transfected with adv-TNAP-OE for 48 h and exposed to hypoxia for 24 h, the results were measure by western blot. n = 4 per group. (**e**) ERK1/2 signaling in cultured CFs transfected with adv-shTNAP for 48 h and incubated with or without TGF-β1 for 24 h. n = 4 per group. (**f**) ERK1/2 signaling in cultured CFs transfected with adv-TNAP-OE for 48 h and incubated with or without TGF-β1 for 24 h. n = 4 per group. Data were expressed as mean ± SEM. One-way ANOVA test was used to test the difference. $^{*}P<0.05$, $^{**}P<0.01$, $^{***}P<0.001$.

level was positively correlated with serum PICP and PIIINP concentrations in patients with MI. The findings supported the hypothesis that TNAP might be a potential biomarker of cardiac fibrosis after MI.

Because TNAP mutations can cause fatal congenital metabolic defects [27], TNAP knockout mice die within 2 weeks after birth [28,29]. The transgenic overexpression of TNAP results in generalized arterial calcification [30], and thus these animal models cannot be used in our experiments. Therefore, we constructed adenovirus-mediated knockdown and overexpression TNAP plasmids to further elucidate the potential role of TNAP in cardiac fibrosis. Consistent

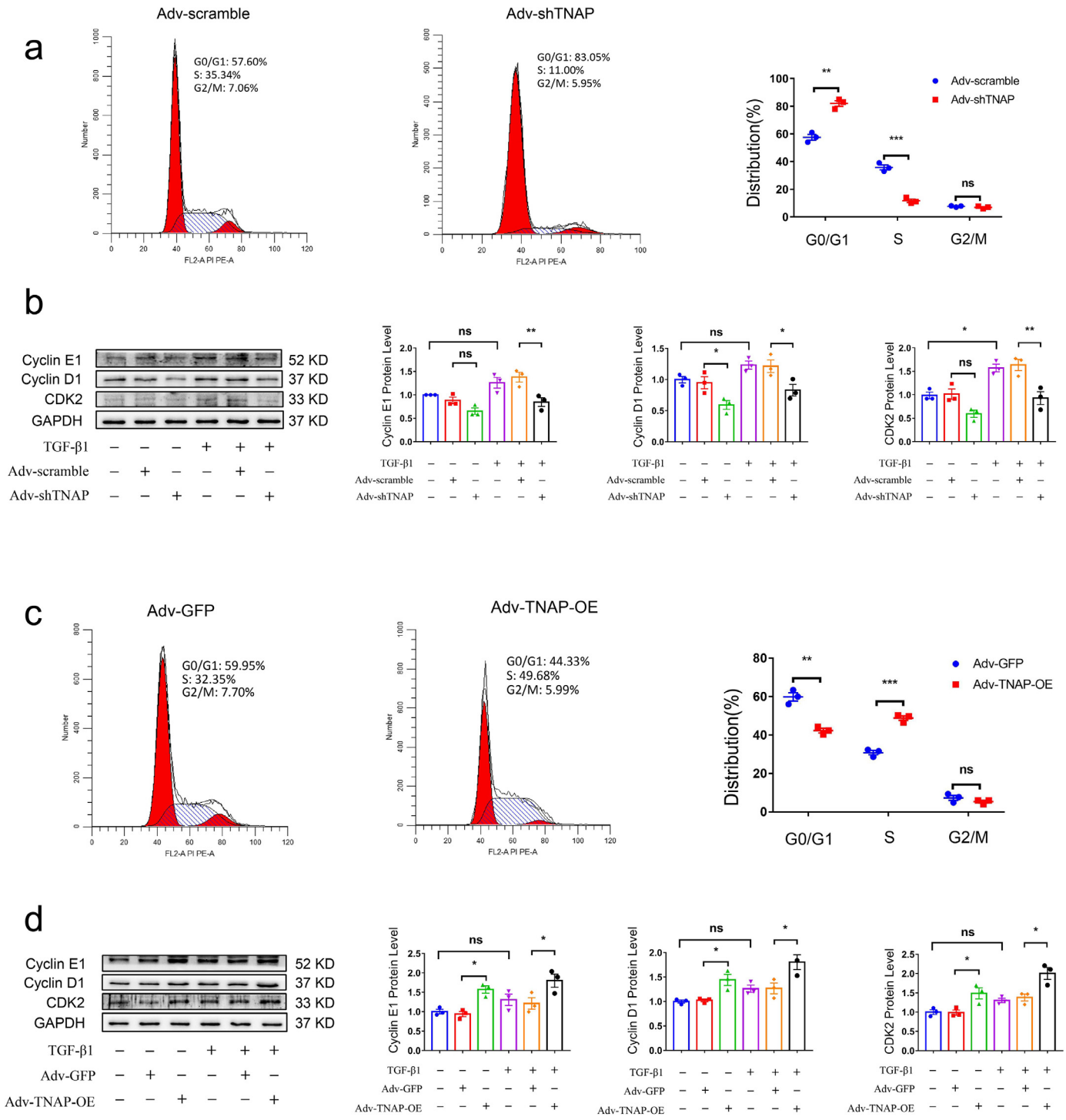

Fig. 7. TNAP promotes the conversion of G1 phase to S phase and regulates the expression of cell cycle proteins in CFs. (**a**) Cell cycle assessed by flow cytometry after transfecting with adv-shTNAP for 48 h. The percentages of each phase cells were analyzed and shown in the right panel. $n = 3$ per group. (**b**) Protein level of cyclin E1, cyclin D1 and CDK2 in cultured CFs transfected with adv-shTNAP were measured by western blot. (**c**) Cell cycle assessed by flow cytometry after transfecting with adv-TNAP-OE for 48 h. The percentages of each phase cells were analyzed and shown in the right panel. $n = 3$ per group. (**d**) Protein level of cyclin E1, cyclin D1 and CDK2 in cultured CFs transfected with adv-TNAP-OE were measured by western blot. $n = 3$ per group. Data were expressed as mean ± SEM. Two-tailed unpaired Student's t-test (a, c) or 1-way ANOVA test (b, d) was used to test the difference. $^{*}P<0.05$, $^{**}P<0.01$, $^{***}P<0.001$.

with previous results [12], TNAP knockdown ameliorated cardiac fibrosis and improved cardiac function. In contrast to these findings, TNAP overexpression aggravated collagen deposition and worsened cardiac function after MI surgery.

The TGF-β1/Smads signaling pathway plays an important role in the activation of CFs [19,31]. As expected, TNAP overexpression increased the levels of TGF-β1 and phosphorylated Smad2/3, whereas the opposite findings were observed in mice injected with adv-shTNAP. Benedetta et al. claimed that by using $TNAP^{cre}Tgf\beta r2^{fl/fl}$ mice and C2C12 myoblasts, TNAP resists TGF-β-dependent cardiac fibrosis by inactivating Smad2/3 [10]. However, the findings of this study only demonstrate that *Tgfβr2* is essential for AngII-induced fibrosis, but the evidence for TNAP-mediated suppression of cardiac fibrosis is insufficient. Rodionov et al. reported that a mouse CAD model with endothelial TNAP overexpression exhibited increased cardiac fibrosis and LVEF [11]. Kermer et al. reported that TNAP

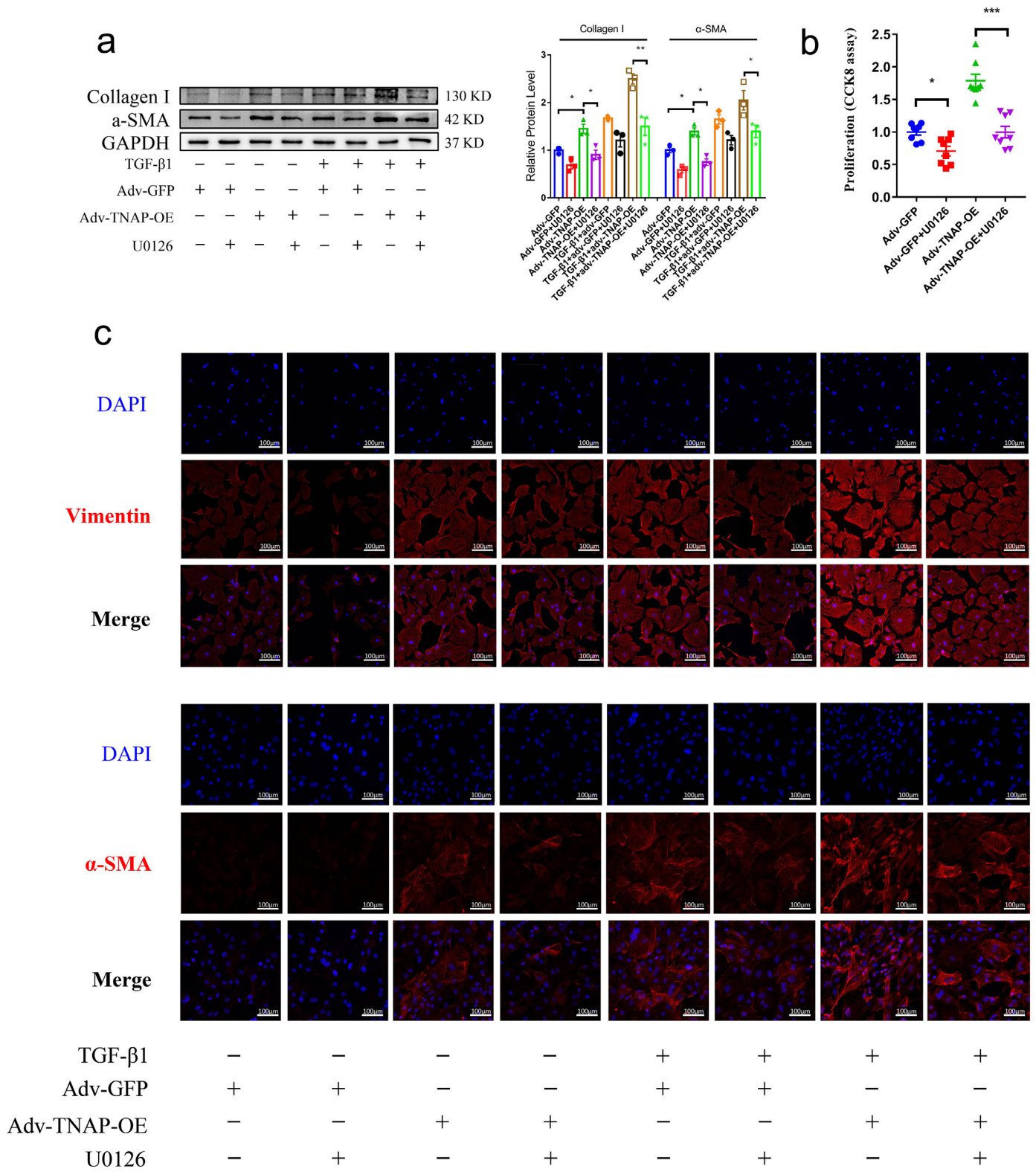

Fig. 8. The inhibition of ERK1/2 signal ameliorates the activation and proliferation of CFs. (**a**) The expression of α-SMA and Collagen I proteins in CFs transfected with adv-TNAP-OE and incubated with TGF-β1 and U0126 (10 μmol/L) were measured by western blot. n = 3 per group. (**b**) CCK-8 proliferation assay of CFs transfected with adv-TNAP-OE and incubated with U0126 for 24 h. n = 8 per group. (**c**) The expression of α-SMA and vimentin in CFs transfected with adv-TNAP-OE and incubated with TGF-β1 and U0126 were measured by immunofluorescence. Data were expressed as mean ± SEM. One-way ANOVA test was used to test the difference. $^{*}P<0.05$, $^{**}P<0.01$, $^{***}P<0.001$.

promotes neural stem cell migration in vitro and possibly in vivo [32]. The results from both studies were consistent with our findings. The same protein may plays distinct roles in different pathological processes. Hence, we cannot entirely exclude the possibility that TNAP may plays distinct roles in different fibrosis models, which requires further study.

The proliferation of CFs is one of the primary mechanisms leading to the progression of cardiac fibrosis [33]. ERK1/2 signaling is the

major mediator of CFs proliferation [34,35]. Consistent with previous reports [20,36], the phosphorylation of ERK1/2 was increased in the MI mouse model. Our data suggested that TNAP overexpression increased the phosphorylation of ERK1/2, while knockdown of TNAP limited the activation of these proteins, which was also confirmed in vitro. Furthermore, incubation with an ERK1/2 specific inhibitor (U0126) attenuated the proliferation and activation of CFs induced by TNAP overexpression. TNAP plays a vital role in hydrolysing inorganic pyrophosphate or adenosine monophosphate to inorganic phosphate (Pi) [37,38]. Pi plays an important role in increasing the proliferation of various cells though ERK1/2 signaling [39,40]. This finding may explain why TNAP promotes the proliferation of CFs. In addition, the stimulation of ERK1/2 signaling by TNAP may be modulated by Pi-independent mechanisms [41], but this hypothesis must be confirmed in the future.

The ERK1/2 signaling pathway is involved in the regulation of multiple cell cycle phases, including G1/S and G2/M transitions [42–44]. In vitro studies showed that TNAP promoted the cell cycle progression of CFs by increasing the number of cells transitioning from G1 phase to S phase and upregulating the expression of cell cycle regulators such as cyclin D1, cyclin E1 and CDK2. This result is consistent with a report showing that TNAP promotes calvarial progenitor cell cycle progression and cytokinesis via ERK1/2 signaling [41].

Our study had several limitations. First, although we examined the role of TNAP in cardiac fibrosis by transfecting cells and heart tissues with adv-shTNAP and adv-TNAP-OE, a more credible approach would be to use CF-specific knockout mice. Second, if we conducted a correlation analysis between serum TNAP levels and cardiac fibrosis expansion confirmed by cardiac magnetic resonance imaging, the results would be more reliable to define TNAP as a potential circulating biomarker of cardiac fibrosis after MI. Finally, because CFs originate from multiple sources, we were unable to determine which origin of the CF fibrotic reaction is mediated by TNAP, or entirely by TNAP.

In summary, we found that TNAP may be a potential regulator of cardiac fibrosis after MI. Mechanistically, we explored the pro-fibrotic role of TNAP in cardiac fibrosis by regulating the TGF-β1/Smads and ERK1/2 signaling pathways. Our research provides a promising therapeutic target for treating cardiac fibrosis after MI.

Author contributions

CXC and ZDY contributed to the design of cell-based and animal experiments. CXC and WLY performed the pooled analysis. WLY and GL were responsible for experiments involving human samples. CXC, WLY, LGX and WXS performed animal surgeries. CXC, WLY and WXS conducted all experimental procedures and collected all data. CXC, CGL and QS analysed the data. CXC and ZDY wrote the manuscript. All authors read and approved the final version of the manuscript.

Data sharing

All data supporting the conclusions of this study are included within the article and its additional file.

Declaration of Competing Interest

Dr Cheng has nothing to disclose. Dr Wang has nothing to disclose. Dr Wen has nothing to disclose. Dr Gao has nothing to disclose. Dr Li has nothing to disclose. Dr Chang has nothing to disclose. Dr Qin has nothing to disclose. Dr Zhang has nothing to disclose.

Acknowledgments

This study was supported by the National Natural Science Foundation of China, 81970203; National Natural Science Foundation of China, 31800976; Chongqing Science and Health Joint Medical Research Project, 2018QNXM024 and Natural Science Foundation of Chongqing, cstc2018jcyjA0153. We thank the Laboratory Research Center of The First Affiliated Hospital of Chongqing Medical University for providing the experimental platform.

Supplementary materials

Supplementary material associated with this article can be found, in the online version, at doi:10.1016/j.ebiom.2021.103370.

References

[1] Jneid H, Addison D, Bhatt DL. 2017 AHA/ACC clinical performance and quality measures for adults with ST-elevation and non-ST-elevation myocardial infarction: a report of the American college of cardiology/American heart association task force on performance measures. J Am Coll Cardiol 2017;70:2048–90.
[2] Prabhu SD, Frangogiannis NG. The biological basis for cardiac repair after myocardial infarction: from inflammation to fibrosis. Circ Res 2016;119:91–112.
[3] González A, Schelbert EB, Díez J, Butler J. Myocardial interstitial fibrosis in heart failure: biological and translational perspectives. J Am Coll Cardiol 2018;71:1696–706.
[4] Haarhaus M, Brandenburg V, Kalantar-Zadeh K, Stenvinkel P, Magnusson P. Alkaline phosphatase: a novel treatment target for cardiovascular disease in CKD. Nat Rev Nephrol 2017;13:429–42.
[5] Ali AT, Penny CB, Paiker JE, Psaras G, Ikram F, Crowther NJ. The effect of alkaline phosphatase inhibitors on intracellular lipid accumulation in preadipocytes isolated from human mammary tissue. Ann Clin Biochem 2006;43:207–13.
[6] Fonta C, Négyessy L, Renaud L, Barone P. Areal and subcellular localization of the ubiquitous alkaline phosphatase in the primate cerebral cortex: evidence for a role in neurotransmission. Cereb Cortex 2004;14:595–609.
[7] Tonelli M, Curhan G, Pfeffer M, et al. Relation between alkaline phosphatase, serum phosphate, and all-cause or cardiovascular mortality. Circulation 2009;120:1784–92.
[8] Park JB, Kang DY, Yang HM, et al. Serum alkaline phosphatase is a predictor of mortality, myocardial infarction, or stent thrombosis after implantation of coronary drug-eluting stent. Eur Heart J 2013;34:920–31.
[9] Korosoglou G, Giusca S, Katus HA. The coronary calcium paradox: yet another step towards the differentiation between stable and rupture-prone coronary plaques? Atherosclerosis 2018;274:232–4.
[10] Arnò B, Galli F, Roostalu U, et al. TNAP limits TGF-β-dependent cardiac and skeletal muscle fibrosis by inactivating the SMAD2/3 transcription factors. J Cell Sci 2019;132:jcs234948.
[11] Rodionov RN, Begmatov H, Jarzebska N, et al. Homoarginine supplementation prevents left ventricular dilatation and preserves systolic function in a model of coronary artery disease. J Am Heart Assoc 2019;8:e012486.
[12] Gao L, Wang LY, Liu ZQ, et al. TNAP inhibition attenuates cardiac fibrosis induced by myocardial infarction through deactivating TGF-β1/Smads and activating P53 signaling pathways. Cell Death Dis 2020;11:44.
[13] Mohammad FK, Faris GA, Rhayma MS, Ahmed K. Neurobehavioral effects of tetramisole in mice. Neurotoxicology 2006;27:153–7.
[14] Nowak LG, Rosay B, Czégé D, Fonta C. Tetramisole and levamisole suppress neuronal activity independently from their inhibitory action on tissue non-specific alkaline phosphatase in mouse cortex. Subcell Biochem 2015;76:239–81.
[15] Shamseer L, Moher D, Clarke M, et al. Preferred reporting items for systematic review and meta-analysis protocols (PRISMA-P) 2015: elaboration and explanation. BMJ 2015;350:g7647.
[16] Wells GA, Shea B, O'Connell D, et al. The Newcastle–Ottawa scale (NOS) for assessing the quality of nonrandomised studies in meta-analyses. Ottawa, Ontario, Canada: Ottawa Hospital Research Institute; 2020 http://www.ohri.ca/programs/clinical_epidemiology/oxford.asp (Augustdate last accessed.
[17] López B, González A, Ravassa S, et al. Circulating biomarkers of myocardial fibrosis: the need for a reappraisal. J Am Coll Cardiol 2015;65:2449–56.
[18] Oatmen KE, Cull E, Spinale FG. Heart failure as interstitial cancer: emergence of a malignant fibroblast phenotype. Heart failure as interstitial cancer: emergence of a malignant fibroblast phenotype. Nat Rev Cardiol 2020;17:523–31.
[19] Khalil H, Kanisicak O, Prasad V, et al. Fibroblast-specific TGF-beta-Smad2/3 signaling underlies cardiac fibrosis. J Clin Invest 2017;127:3770–83.
[20] Liu Z, Xu Q, Yang Q, et al. Vascular peroxidase 1 is a novel regulator of cardiac fibrosis after myocardial infarction. Redox Biol 2019;22:101151.
[21] Li P, Liu P, Peng Y, et al. The ERK/CREB pathway is involved in the c-Ski expression induced by low TGF-β1 concentrations during primary fibroblast proliferation. Cell Cycle 2018;17:1319–28.
[22] Augé N, Maupas-Schwalm F, Elbaz M, et al. Role for matrix metalloproteinase-2 in oxidized low-density lipoprotein-induced activation of the sphingomyelin/ceramide pathway and smooth muscle cell proliferation. Circulation 2004;110:571–8.
[23] Ndrepepa G, Xhepa E, Braun S, et al. Alkaline phosphatase and prognosis in patients with coronary artery disease. Eur J Clin Invest 2017;47:378–87.
[24] Yu T, Jiao Y, Song J, et al. Prognostic impact of alkaline phosphatase for in-hospital mortality in patients with acute coronary syndrome: a prospective cohort study in China. BMJ Open 2019;9:e025648.

[25] Puls M, Beuthner BE, Topci R, et al. Impact of myocardial fibrosis on left ventricular remodelling, recovery, and outcome after transcatheter aortic valve implantation in different haemodynamic subtypes of severe aortic stenosis. Eur Heart J 2020;41:1903–14.
[26] Ho CY, López B, Coelho-Filho OR, et al. Myocardial fibrosis as an early manifestation of hypertrophic cardiomyopathy. N Engl J Med 2010;363:552–63.
[27] Liu J, Nam HK, Campbell C, Gasque KC, Millán JL, Hatch NE. Tissue-nonspecific alkaline phosphatase deficiency causes abnormal craniofacial bone development in the Alpl(-/-) mouse model of infantile hypophosphatasia. Bone 2014;67:81–94.
[28] Waymire KG, Mahuren JD, Jaje JM, Guilarte TR, Coburn SP, MacGregor GR. Mice lacking tissue non-specific alkaline phosphatase die from seizures due to defective metabolism of vitamin B-6. Nat Genet 1995;11:45–51.
[29] Sebastian-Serrano A, Engel T, De Diego-Garcia L, et al. Neurodevelopmental alterations and seizures developed by mouse model of infantile hypophosphatasia are associated with purinergic signalling deregulation. Hum Mol Genet 2016;25:4143–56.
[30] Savinov AY, Salehi M, Yadav MC, Radichev I, Millán JL, Savinova OV. Transgenic overexpression of tissue-nonspecific alkaline phosphatase (TNAP) in vascular endothelium results in generalized arterial calcification. J Am Heart Assoc 2015;4.
[31] Rainer PP, Hao S, Vanhoutte D, et al. Cardiomyocyte-specific transforming growth factor β suppression blocks neutrophil infiltration, augments multiple cytoprotective cascades, and reduces early mortality after myocardial infarction. Circ Res 2014;114:1246–57.
[32] Kermer V, Ritter M, Albuquerque B, Leib C, Stanke M, Zimmermann H. Knockdown of tissue nonspecific alkaline phosphatase impairs neural stem cell proliferation and differentiation. Neurosci Lett 2010;485:208–11.
[33] Zhang W, Liu H. MAPK signal pathways in the regulation of cell proliferation in mammalian cells. Cell Res 2002;12:9–18.
[34] Hu J, Wang X, Wei SM, Tang YH, Zhou Q, Huang CX. Activin A stimulates the proliferation and differentiation of cardiac fibroblasts via the ERK1/2 and p38-MAPK pathways. Eur J Pharmacol 2016;789:319–27.
[35] Nguyen QT, Nsaibia MJ, Sirois MG, et al. PBI-4050 reduces pulmonary hypertension, lung fibrosis, and right ventricular dysfunction in heart failure. Cardiovasc Res 2020;116:171–82.
[36] Oba T, Yasukawa H, Hoshijima M, et al. Cardiac-specific deletion of SOCS-3 prevents development of left ventricular remodeling after acute myocardial infarction. J Am Coll Cardiol 2012;59:838–52.
[37] Andrade CM, Roesch GC, Wink MR, et al. Activity and expression of ecto-5′-nucleotidase/CD73 are increased during phenotype conversion of a hepatic stellate cell line. Life Sci 2008;82:21–9.
[38] Davidson JA, Urban T, Tong S, et al. Alkaline phosphatase, soluble extracellular adenine nucleotides, and adenosine production after infant cardiopulmonary bypass. PLoS ONE 2016;11:e0158981.
[39] Khalid S, Yamazaki H, Socorro M, Monier D, Beniash E, Napierala D. Reactive oxygen species (ROS) generation as an underlying mechanism of inorganic phosphate (P)-induced mineralization of osteogenic cells. Free Radic Biol Med 2020;153:103–11.
[40] Tan X, Xu X, Zeisberg EM, Zeisberg M. High inorganic phosphate causes DNMT1 phosphorylation and subsequent fibrotic fibroblast activation. Biochem Biophys Res Commun 2016;472:459–64.
[41] Nam HK, Vesela I, Siismets E, Hatch NE. Tissue nonspecific alkaline phosphatase promotes calvarial progenitor cell cycle progression and cytokinesis via Erk1,2. Bone 2019;120:125–36.
[42] Moniz S, Veríssimo F, Matos P, et al. Protein kinase WNK2 inhibits cell proliferation by negatively modulating the activation of MEK1/ERK1/2. Oncogene 2007;26:6071–81.
[43] Romanov V, Whyard TC, Waltzer WC, Grollman AP, Rosenquist T. Aristolochic acid-induced apoptosis and G2 cell cycle arrest depends on ROS generation and MAP kinases activation. Arch Toxicol 2015;89:47–56.
[44] Dumesic PA, Scholl FA, Barragan DI, Khavari PA. Erk1/2 MAP kinases are required for epidermal G2/M progression. J Cell Biol 2009;185:409–22.